Supporting Information

Pandey et al. 10.1073/pnas.1110857108

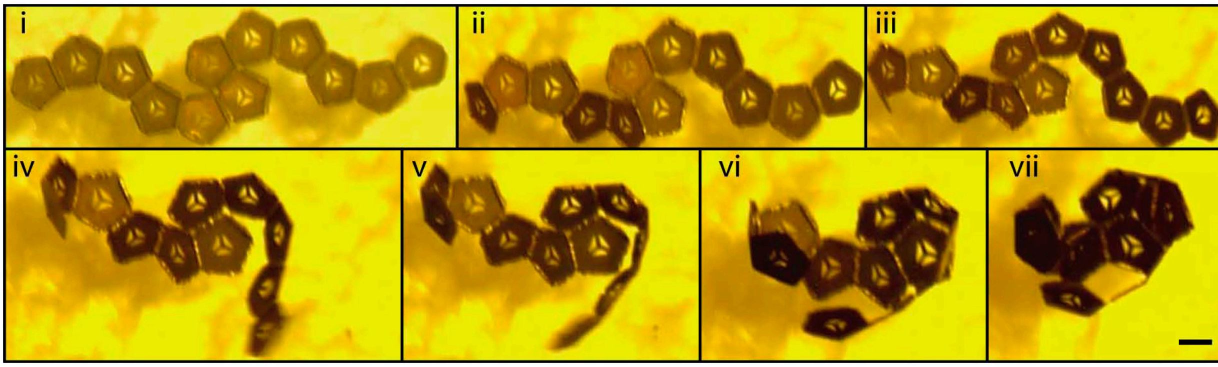

Fig. S1. Folding pathway for the dodecahedron (V_c). Optical microscopy images showing a folding pathway of a dodecahedral net with $V_c = 2$ as in Fig. 2*A*.

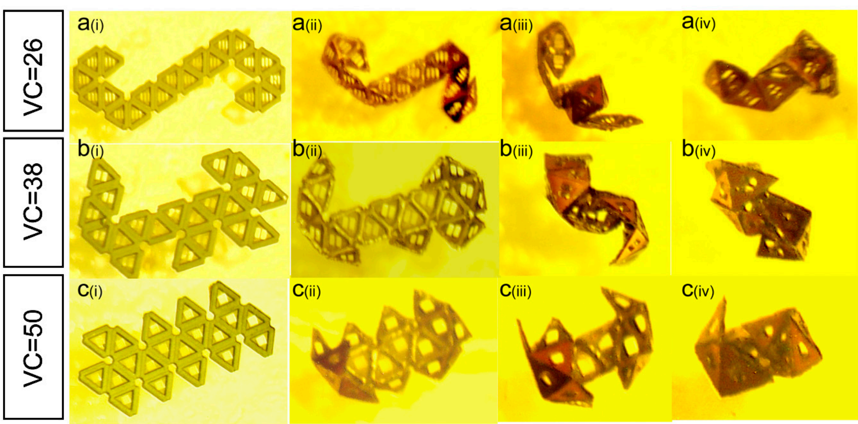

Fig. S2. Folding pathways for the icosahedron. Optical microscopy images showing folding pathways of icosahedral nets with 3D structure for the icosahedron. *A i–iv*, $V_c = 26$; *Bi–iv*, $V_c = 38$; *C i–iv*, $V_c = 50$.

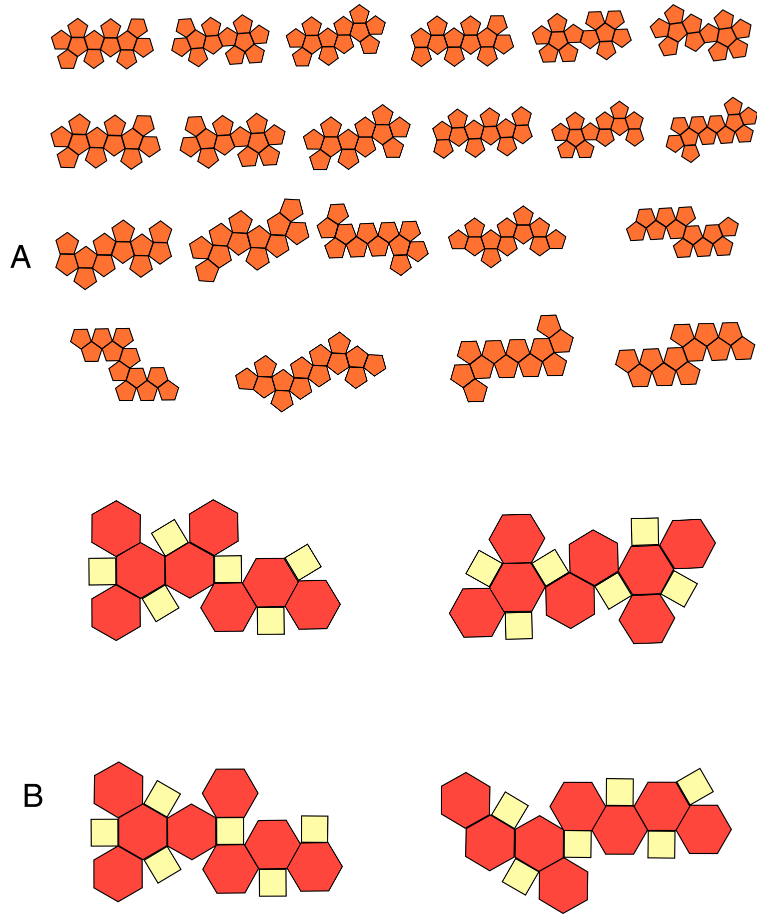

Fig. S3. (*A*) High V_c nets for the dodecahedron. All $V_c = 10$ nets (21 out of all 43,380) arranged in order of increasing R_g; (*B*) High V_c nets for the truncated octahedron. All $V_c = 4$ nets (four out of the 123,452 nets found) are shown.

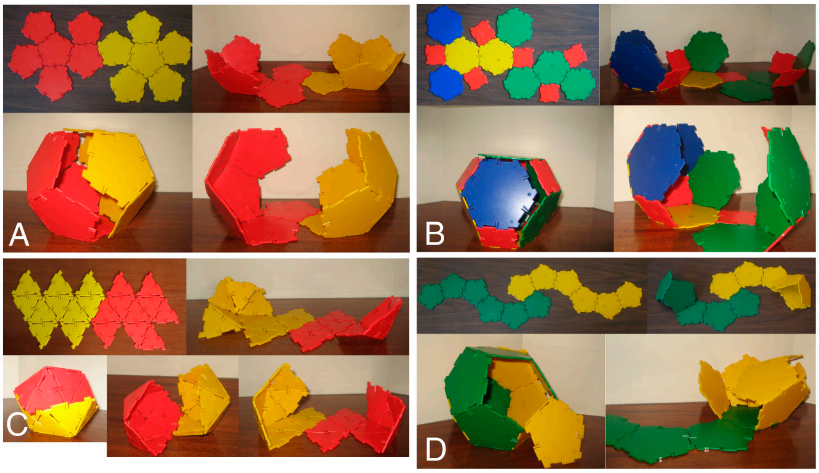

Fig. S4. Models illustrating the gluing at vertex connections algorithm. Manually folded centimeter-scale models. (*A*) $V_c = 10$ dodecahedron; (*B*) $V_c = 12$ truncated octahedron; (*C*) $V_c = 50$ icosahedron; (*D*) $V_c = 2$ dodecahedron. *A–C* are high V_c nets. They have the common feature that the penultimate intermediate consists of two mating halves. The same intermediates are also see in experiments with these nets for the dodecahedron and truncated octahedron and also in computed geodesics. However, these halves are rigid only for *A* and *B*. Both *C* and *D* are not rigid. The five-valent vertices in *C*, though fully formed, are not rigid. *D* has long floppy segments that lead to misaligned structures. Surprisingly, it does yield some "B-grade" specimens (see Figs. 2 and 4).

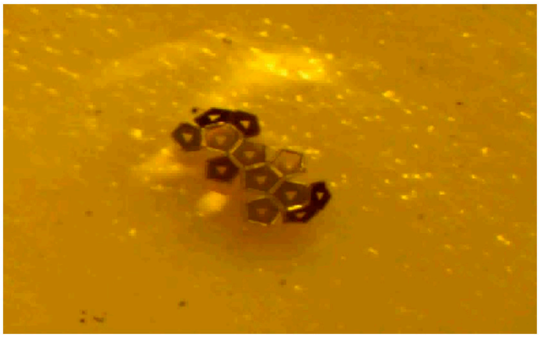

Movie S1. Folding pathway for the dodecahedron ($V_c = 10$). Optical microscopy movie of self-folding for a dodecahedral net with $V_c = 10$ as in Fig 2*C*.
Movie S1 (WMV)

Table S1. Yields for all 300-μm dodecahedron nets

Net	%A	%B	%C
$V_c = 2$	0	14	86
$V_c = 6$	16	34	50
$V_c = 10$	34	44	22
$R_g = 1,102.2$ μm	0	8	92
$R_g = 800.9$ μm	4	10	86
$R_g = 693.7$ μm	6	16	78

Fifty samples were tested for each net.

Table S2. Yields for all 300-μm truncated octahedron nets

Net	%A	%B	%C
$V_c = 2$	0	0	100
$V_c = 7$	0	22	78
$V_c = 12$	24	34	42
$R_g = 1,306.3$ μm	0	0	100
$R_g = 912.7$ μm	0	18	82
$R_g = 795.0$ μm	12	22	66

Fifty samples were tested for each net.

Table S3. Yields of 300-μm dodecahedron nets with same number of vertex connections ($V_c = 10$) and different radius of gyration (R_g)

Net, μm	%A	%B	%C
$R_g = 810.2$	8	56	36
$R_g = 797.4$	8	60	32
$R_g = 755.4$	22	50	28
$R_g = 747.7$	20	62	18

Table S4. Yields of 300-μm truncated octahedron nets with same number of vertex connections ($V_c = 12$) and different radius of gyration (R_g)

Net, μm	%A	%B	%C
$R_g = 911.6$	16	30	54
$R_g = 870.2$	22	24	54
$R_g = 867.4$	20	28	52
$R_g = 852.8$	30	38	32